View metadata, citation and similar papers at core.ac.uk

brought to you by CORE

provided by IntechOpen

We are IntechOpen, the world's leading publisher of Open Access books Built by scientists, for scientists

4,800
Open access books available

122,000
International authors and editors

135M
Downloads

Our authors are among the

154
Countries delivered to

TOP 1%
most cited scientists

12.2%
Contributors from top 500 universities

CLARIVATE ANALYTICS BOOK CITATION INDEX INDEXED

WEB OF SCIENCE™

Selection of our books indexed in the Book Citation Index in Web of Science™ Core Collection (BKCI)

Interested in publishing with us?
Contact book.department@intechopen.com

Numbers displayed above are based on latest data collected.
For more information visit www.intechopen.com

17

Some Techniques in Configurational Geometry as Applied to Solar Collectors and Concentrators

Reccab M Ochieng and Frederick N Onyango
Department of Physics and Materials Science, Maseno University,
P.O. Box 333, Maseno 40105,
Kenya

1. Introduction

All systems, which harness and use the sun's energy as heat, are called solar thermal systems. These include solar water heaters, solar air heaters, and solar stills for distilling water, crop driers, solar space heat systems and water desalination systems.

This chapter presents analysis based on configurational geometry of solar radiation collectors and concentrators using system models that have the same dimensions, material structure and properties. The work shows that different elements added to concentrators of well known configurations increase the geometric concentration ratio.

The need to develop effective solar thermal systems is not only to reduce the effects of global warming but also to reduce the overall costs and risks of climate change. Therefore, it is paramount to develop technologies for utilizing clean and renewable energy on a large scale.

Solar energy being the cleanest source of renewable energy free of Green House Gas (GHG) emission has seen the development of many gadgets and new technologies which include power generation (e.g., photovoltaic and solar thermal), heating, drying, cooling, ventilation, etc.

Development of the technologies utilizing solar energy focuses on improving the efficiency and reducing the cost. The objective of this book chapter is to present an analysis based on configurational geometry of solar radiation collectors and concentrators using system models that have been used to demonstrate the technique of configurational geometry in design and applications of a number of systems.

Geometry configuration plays an important role in most if not all solar collectors and concentrators. A number of collectors and concentrators have symmetries which allow them to collect and concentrate solar thermal energy. Since solar collector and concentrator surfaces are normally planes or curves of specific configurations, the analysis of system processes can be carried out through the use of the laws and rules of optics. Because of the known geometries and symmetries found in the collectors and concentrators, analysis of the collection and reflection of light, hence radiation analysis can also be done using configurational geometries of the systems. We shall discuss the general principles of operation of solar collectors and concentrators then show in a number of ways that it is possible to design collectors and concentrators innovatively using the method of configurational geometry. By use of some

examples, we shall show the importance and effect of configurational geometry on the Geometric Concentartion Ratio, CR_g, of a concentrator, defined as the area of the collector aperture A_a, divided by the surface area of the receiver, A_r (Garg & Kandpal, 1978). We show that for given dimensions of a specific solar collector and concentrator system, (a modified cone concentrator and a modified inverted cone concentrator), the configurational geometries give different concentration ratios unless certain conditions are prescribed. We also demonstrate that different new elements and components can be incorporated in well known configurational geometries to improve the performance of collectors and concentrators. In this chapter, we first give a brief discussion on the general aspects of concentrators and collectors which is then followed by

a. a mathematical procedure in concentrators and collectors with respect to configurational geometry,
b. a technique of generating cone concentrators and collectors from hyperbloid configurations,
c. a discussion of configurational geometry in straight cone concentrators and inverted cone concentrators and collectors and.

2. General theoretical considerations

A typical flat plate collector consists of an absorber plate, one or more transparent cover(s), thermal insulation, heat removal system and an outer casing.

An absorber plate is generally a sheet of metal of high thermal conductivity like copper which is normally coated with black paint or given a special coating (called selective coating) so that it absorbs the incident solar radiation efficiently and minimizes loss of heat by radiation from the collector plate.

In the flat plate solar collector, a glass plate of good quality, which is transparent to incoming solar radiation to act as cover, is fixed about 2-4 cm above the absorber plate. This prevents convective heat loss from the absorber plate and prevents infrared radiation from the plate escaping to the atmosphere. If the plate temperature under normal operation is expected to be higher than 80^0C, two glass plates separated from each other may be used.

The absorber plate rests on a 5-15 cm thick bed of glass wool or any other good thermally insulating material of adequate thickness, which is also placed along the sides of the collector plate to cut down heat loss by conduction.

The most common method of removing heat from the collector plate is by fixing tubes, called risers at spacing of about 10-25 cm. Good thermal contact between the tube and plate is very important for efficient operation of the collector hence the tubes could be soldered, spot welded, tied with wires or clamped to the plate. These risers are connected to larger pipes called headers at both ends so that heat removal fluid can enter from the lower header and leave from the upper header. This configuration of absorber plate is called the fin type and is most commonly used. The heat removal fluid, usually water or oil, flows through these tubes to carry away the heat received from the sun. In another type of collector, heat removal fluid flows between two sheets of metal sealed at the edges, the top acting as the absorber plate.

All parts of the collector are kept in an outer case usually made of metal sheets. The case is made air tight to avoid considerable loss of heat from the collector plate to the ambient.

The collector is finally placed on a stand so that the absorber plate is correctly inclined to the horizontal and receives maximum amount of heat from the sun during a particular season or the entire year.

Flat plate solar collectors may be divided into two main classifications based on the type of heat transfer fluid used. Either liquid or gases (most often air) is used in collectors. Liquid heating collectors are used for heating water and non-freezing aqueous solutions and occasionally for non-aqueous heat transfer liquids such as thermal oils, ethylene glycol e.t.c,. Air-heating collectors are used for heating air used for solar dying or space heating (such as rooms).

Many advanced studies both experimental and theoretical have been carried out on flat plate solar collectors. Accurate modelling of solar collector system using a rigorous radiative model applied for the glass cover, which represents the most important component, has been reported by (Maatouk & Shigenao, 2005).

A different category of solar thermal systems known as solar concentrators are also used in solar thermal systems. Solar concentrators are the collection of devices which increase solar radiation flux on the absorber surface as compared to the radiation flux existing on the entrance aperture. Figure 1 show schematic diagrams of the most common conventional configurations of concentrating solar collectors. Optical concentration is achieved by the use of reflecting or refracting elements positioned to concentrate the incoming solar radiation flux onto a suitable absorber. Due to the apparent diurnal motion of the sun, the concentrating surface, whether reflecting or refracting will not be in a position to redirect the solar radiation on the absorber throughout the day if both the concentrator surface and absorber are stationary. This requires the use of a tracking system.

Ideally, the total system consisting of mirror/lens and absorber should follow the sun's apparent motion so that the sun rays are always captured by the absorber. In general, therefore, a solar concentrator consists of (i) a focusing device (ii) a blackened metallic absorber provided with a transparent cover and (iii) a tracking device for continuously following the sun. Temperatures as high as $3{,}000^0$C can be achieved with solar concentrators which find applications in both photo-thermal and photovoltaic conversion of solar energy.

The use of solar concentrators may lead to advantages such as increase energy delivery temperatures, improved thermal efficiency due to reduced heat loss, reduced cost due to replacement of large quantities of expensive material(s) for constructing flat plate solar collector systems by less expensive reflecting and/or refracting elements and a smaller absorber tube. Additionally there is the advantage of increased number of thermal storage options at elevated temperatures thus reducing the storage cost. Earlier works by (Morgan 1958), (Cornbleet, 1976), (Basset & Derrick, 1978), (Burkhard & Shealy, 1975), (Hinterberger & Winston, 1968a), (Rabl 1976a, 1976b, 1976c), (Rabl & Winston, 1976), provide some important information and ideas on the development and design of solar collectors and concentrators as employed in this work.

The use of optical devices in solar concentrators makes it necessary that some of the parameters characterizing solar concentrators are different than those used in flat plate solar collectors. Several terms are used to specify concentrating collectors. These are:

i. Aperture area
ii. Acceptance angle
iii. Absorber area
iv. Geometric concentration ratio
v. Local concentration ratio
vi. Intercept factor
vii. Optical efficiency
viii. Thermal efficiency.

The aperture area, A_a, is defined as the plane area through which the incident solar radiation is accepted whereas the acceptance angle $(\theta_{\max})$ defines the limit to which the incident ray path may deviate from the normal drawn to the aperture plane and still reach the absorber. A concentrator with large acceptance angle needs only seasonal adjustments while one with small acceptance angle must track the sun continuously.

The absorber area (A_{abs}), is the total area that receives the concentrated solar radiation. It is the area from which useful energy can be removed and the geometric concentration ratio (CR_g), or the radiation balance concentration ratio of a solar concentrator is defined as the ratio of the collecting aperture area (A_{Ap}), to the area of the absorber (A_{abs}). Mathematically this is given by

$$(CR_g) = \frac{A_{Ap}}{A_{abs}} \tag{2.1}$$

The brightness concentration ratio or the local concentration ratio is a quantity that characterizes the nonuniformity of illumination over the surface of the absorber.

It is the ratio of the radiation flux arriving at any point on the absorber to the incident radiation flux at the entrance aperture of the solar concentrator. In some literature, the brightness ratio is called optical concentration ratio (CR_o) and is defined as the average irradiance (radiant flux) (I_r) integrated over the receiver area (A_r) divided by the insolation incident on the collector aperture. Mathematically, this takes the form

$$CR_o = \frac{\frac{1}{A_r}\int I_r dA_r}{I_a} \tag{2.2}$$

The intercept factor (γ) for a concentrator-receiver system is defined as the ratio of energy intercepted by the absorber of a chosen size to the total energy reflected/refracted by the focusing device, that is,

$$\gamma = \frac{\int_{-\omega/2}^{+\omega/2} I(x)dx}{\int_{-\infty}^{+\infty} I(x)dx} \tag{2.3}$$

where $I(x)$ is the solar flux at a certain position (x) and ω is the width of the receiver. For a typical concentrator-receiver design its value depends on the size of the absorber, the surface area of the concentrator and solar beam spread.

The optical efficiency (η_0), of a solar concentrator-receiver system is defined as the ratio of the energy absorbed by the absorber to the energy incident on the concentrator's aperture. It includes the effect of mirror/lens surface shape and reflection/transmission losses, tracking accuracy, shading, receiver cover transmittance of the absorber and solar beam incidence effects.

In a thermal conversion system, a working fluid may be a liquid, a vapour or gas is used to extract energy from the absorber. The thermal performance of a solar concentrator is characterized by its thermal efficiency, which is defined as the ratio of useful energy delivered to the energy incident on the aperture of the concentrator.

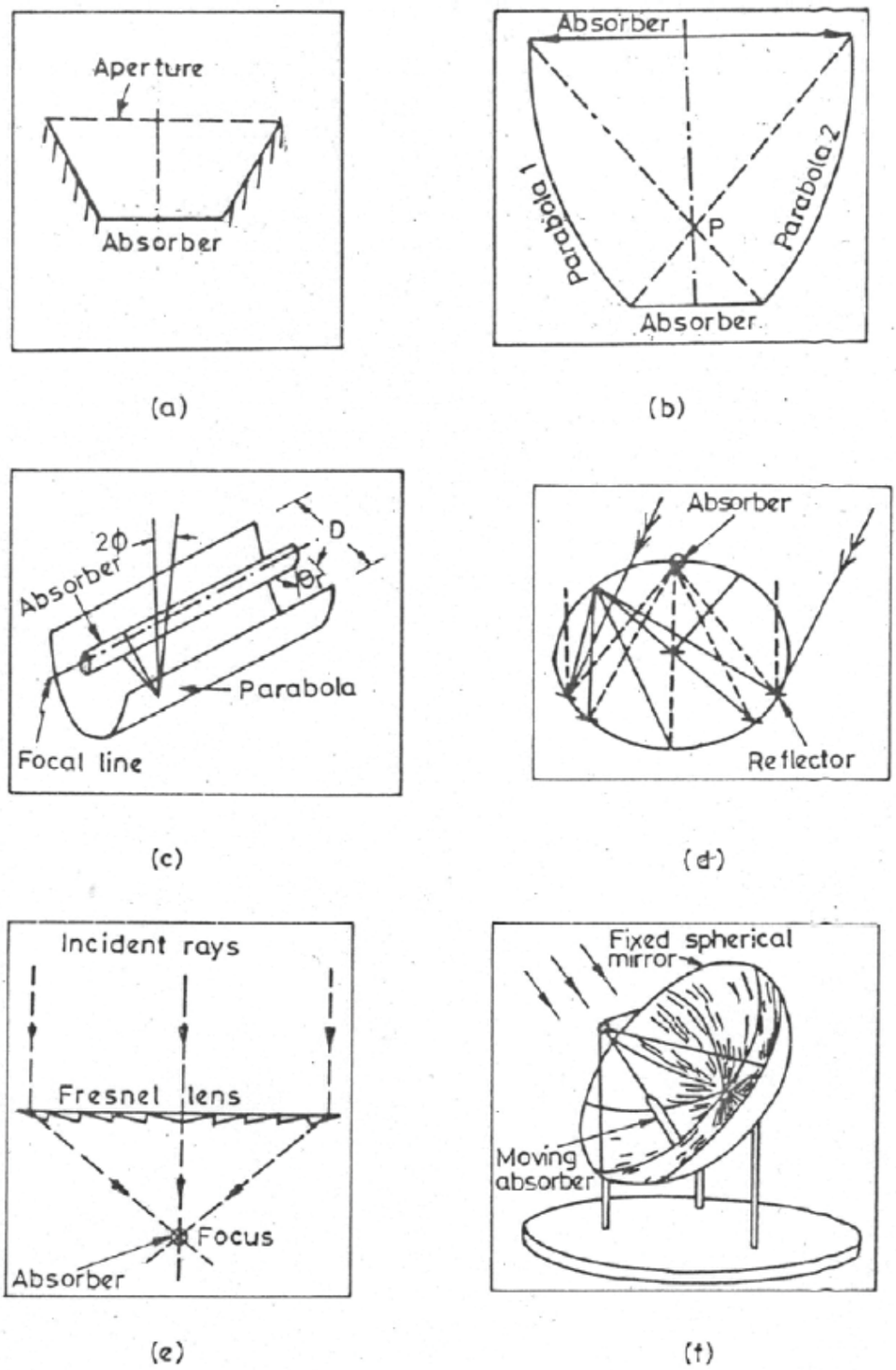

Fig. 1.1. *Schematic diagrams of the most common solar concentrators: (a) Flat plate absorber with plane reflectors (V trough), (b) compound parabolic concentrator, (c) Cylindrical parabolic trough, (d) Russel's fixed mirror solar concentrator, (e) Fresnel lens, (f) Hemispherical bowl. (Adopted from Garg and Kandpal, 1999).*

The instantaneous efficiency of a solar concentrator may be calculated from an energy balance on the absorber. The useful energy delivered by a concentrator is given by

$$Q = \eta_0 I_b A_a - U_L (T_{abs} - T_a) A_{abs} \tag{2.4}$$

where I_b is the direct beam on the concentrator, U_L is called the overall heat loss coefficient for the collector of the concentrator and is the sum for the heat loss from the bottom, U_b, the sides, U_s, and the top, U_t, i.e.,

$$U_L = U_b + U_s + U_t \,. \tag{2.5}$$

The other symbols have their usual meanings as previously defined. In situations where the receiver is not protected by a transparent cover, the useful heat collected by the receiver Q can be calculated as,

$$Q = A_{Ap} \cdot \left(\alpha \cdot C \cdot E^S - \varepsilon \cdot \sigma \cdot T_A^4 - U_L \left(T_A - T_a \right) \right) \tag{2.6}$$

with $\left(A_{Ap} \right)$ being the entrance aperture area, α being the absorptivity of the absorber with respect to the solar spectrum, (C) the concentration factor, E^S, the radiation density of the direct solar radiation and ε the average emissivity of the absorber with respect to the black body radiation at the absorber temperature T_A. σ stands for the Stefan-Boltzmann constant whereas U_L is the heat loss coefficient due to convection and conduction. In Eq. (2.6), thermal radiation input from the ambient (with the ambient temperature T_a) to the receiver is neglected.

Taking into account that for the heat transfer from the absorber to the heat transfer fluid a temperature difference is required, the following expression is also valid for the useful energy:

$$Q = A_{Abs} \cdot U_I \cdot \left(T_A - T_F \right) \tag{2.7}$$

with U_I being the inner heat transfer coefficient from the absorber to the fluid, T_F being the average temperature of the heat transfer fluid and A_{Abs} being the absorber area. Using Eq. (2.6) and Eq. (2.7), the energy balance equation can be rewritten replacing the absorber temperature by the fluid temperature:

$$Q = A_{Ap} \cdot \left(F \cdot \alpha \cdot C \cdot E^S - F \cdot \varepsilon \cdot \sigma \cdot T_F^4 - F \cdot U_L \cdot (T_F - T_a) \right) \tag{2.8}$$

The parameter *F* is the heat removal factor and is defined from the energy balance of flat plate solar collectors as

$$F = \frac{A_{Abs} \cdot U_I}{A_{Abs} \cdot U_I + A_{Ap} \cdot U_L + A_{Ap} \cdot 4 \cdot \sigma \cdot T_F^3} \tag{2.9}$$

The thermal efficiency of the receiver, η_{th}, is defined by the ratio of the useful heat to the incoming solar radiation in the aperture. The resulting expression for the efficiency is

$$\eta_{th} = \frac{Q}{A_{Ap} \cdot C.E^S} = F \cdot \alpha - \frac{F \cdot \varepsilon \cdot \sigma \cdot T_F^4}{C \cdot E^S} - \frac{F \cdot U_L \cdot (T_F - T_a)}{C \cdot E^S} \tag{2.10}$$

Using Eq. (2.4) and Eq. (2.5), the instantaneous efficiency of a concentrator having a top cover may be written as

$$\eta = \frac{Q}{I_b A_a} = \eta_0 - \frac{U_L\left(T_{abs} - T_a\right)}{I_b C}. \tag{2.11}$$

The linear approximation of heat loss factor made in Eq. (2.5) for a concentrator with top cover is valid for small operating temperatures only. At high operating temperatures, where the radiation loss term dominates the convective losses, energy balance may be expressed as

$$Q = \eta_0 I_b A_a - U_L(T_{abs}^4 - T_a^4)A_{abs} \tag{2.12}$$

where U_L now takes into account the accompanying convective and conduction losses also, hence Eq. (2.11) may now be modified as

$$\eta = \eta_0 - \frac{U_L\left(T_{abs}^4 - T_a^4\right)}{I_b C}. \tag{2.13}$$

Since the absorber surface temperature is difficult to determine, it is convenient to express the efficiency in terms of the inlet fluid temperature T_i by means of the heat removal factor F as

$$\eta = F\left[\eta_0 - \frac{U_L\left(T_i - T_a\right)}{I_b C}\right]. \tag{2.14}$$

Comparing Eq. (2.10) and Eq. (2.14) one sees that there is a parallel between the "static" efficiency $\left(\eta_0\right)$, the emissivity and the absorptivity of the concentrator. Eq. (2.14) is a first order steady state expression for the instantaneous efficiency of a solar concentrator having a top cover. The instantaneous efficiency of a solar concentrator receiver system is dependent on two types of quantities, namely the concentrator receiver design parameters and the parameters characterizing the operating conditions. The optical efficiency, heat loss coefficient and heat removal factor are the design dependent parameters while the solar flux, inlet fluid temperature and the ambient temperature define the operating conditions.

Geometric optics is used as the basic tool in designing almost any optical system, image-forming or not. Intuitive ideas of a ray of light, roughly defined as the path along which light energy travels together with surfaces that reflect or transmit light are often used in solar collector and concentrator designs. When light is reflected from a smooth surface it obeys the well-known law of reflection which states that the incident and reflected rays make equal angles with the normal to the surface and that both rays lie in one plane.

When light is transmitted, the ray direction is altered according to the law of refraction, Snell's law which states that the sine of the angle between the normal and the incident ray gives a constant ratio to the sine of the angle between the normal and the refracted ray, all the three directions being coplanar.

A major part of design and analysis of solar collectors and concentrators involves ray tracing, i.e., following the paths of rays through a system of reflecting and refracting surfaces. The result of such processes may or may not create images of the source of the ray. Depending on the surface structure, properties and materials used, two types of systems;

image-forming concentrators and non image-forming concentrators arise. The process of ray tracing is used extensively in lens design, but the requirements are somewhat different for concentrators. In conventional lens design, the reflecting or refracting surfaces involved are almost always portions of spheres and centers of spheres lie in one straight line (axisymmetric optical system), so the special methods that take advantage of the simplicity of forms of surfaces and symmetry can be applied.

Nonimaging concentrators do not, in general, have spherical or symmetric surfaces. In fact, sometimes, there are no explicit analytical forms for the surfaces, although there is usually an axis or a plane of symmetry and ray-tracing schemes are conveniently based on vector formulations. Detailed analyses are often dealt with in computer programs on the basis of each different shape.

In principle, the use of ray tracing tells us all there is to know about the geometric optics of a given optical system, image forming or not. However, ray tracing alone is often little or no use for inventing new systems having properties for a given purpose. We need to have ways of describing the properties of optical systems in terms of general performance, using parameters such as, for example, the concentration ratios. A primitive form of nonimaging concentrator, the light cone has been used for many years (see for example, (Hotler *et.al*. 1962), (Witte, 1965), (Williamson, 1952), (Welford & Winston, 1978).

The option to integrate cost effective storage systems directly into solar thermal facilities represents a significant advantage of solar thermal systems over other concepts using renewable energy sources. This idea shall also be discussed with reference to configurational geometry of cone cylinder combination concentrators and collectors.

In the evaluation or calculation of the geometric concentration ratio of most concentrators, standard methods have been employed. This work departs from the traditional approach and outlines the mathematical foundation for such calculations. It will be shown that using the mathematical technique, for a straight cone with a collector area A_{coll}, situated a distance H_2 from the apex and an absorber area, A_{abs}, at a distance H_1 from the apex, the ratio of the squares of H_2 to H_1 give the geometric concentration ratio of the cone concentrator.

3. Mathematical procedures in concentrators and collectors with respect to configurational geometry

In the evaluation or calculation of the geometric concentration ratio of most concentrators, standard methods have been employed. This work departs from the traditional approach and outlines the mathematical foundation for such calculations. We then proceed to determine the concentration ratio of a modified cone concentrator.

The work shows that for a straight cone with a collector area A_{coll}, situated a distance H_2 from the apex and an absorber area, A_{abs}, at a distance H_1 from the apex, the ratio of the squares of H_2 to H_1 give the geometric concentration ratio of the cone concentrator (Figure 3.1).

Figure 3.2 shows a mall elemental volume of a cone that has been generated from a CPC. If the cone subtends an angle $\delta\theta$ and $\delta\phi$ at the origin, its cross-sectional area at a distance r from the apex is $r^2 \sin\theta\delta\theta\delta\phi$. Let us cut a cross section of the cone a distance H_1 from the origin so that the elemental area given by

$$dA_{abs} = H_1^2 \sin\theta\delta\theta\delta\phi \tag{3.1}$$

acts as the absorber area or the exit aperture for a cone concentrator.
Extending the length a distance H_2 from the apex we obtain an elemental collector area or entrance aperture, dA_{coll}, given by

$$dA_{coll} = H_2^2 \sin\theta \delta\theta\delta\phi \tag{3.2}$$

Where $H_2 > H_1$.
From Eq. (3.1) and (3.2) the "elemental" geometric concentration ratio is given by

$$\Delta C_g = \frac{dA_{coll}}{dA_{abs}} = \frac{H_2^2}{H_1^2} \tag{3.3}$$

We shall now explore the calculation of the geometric concentration ratio from the point of view of the relation between the area of a surface of revolution and the length of the curve that generates it.

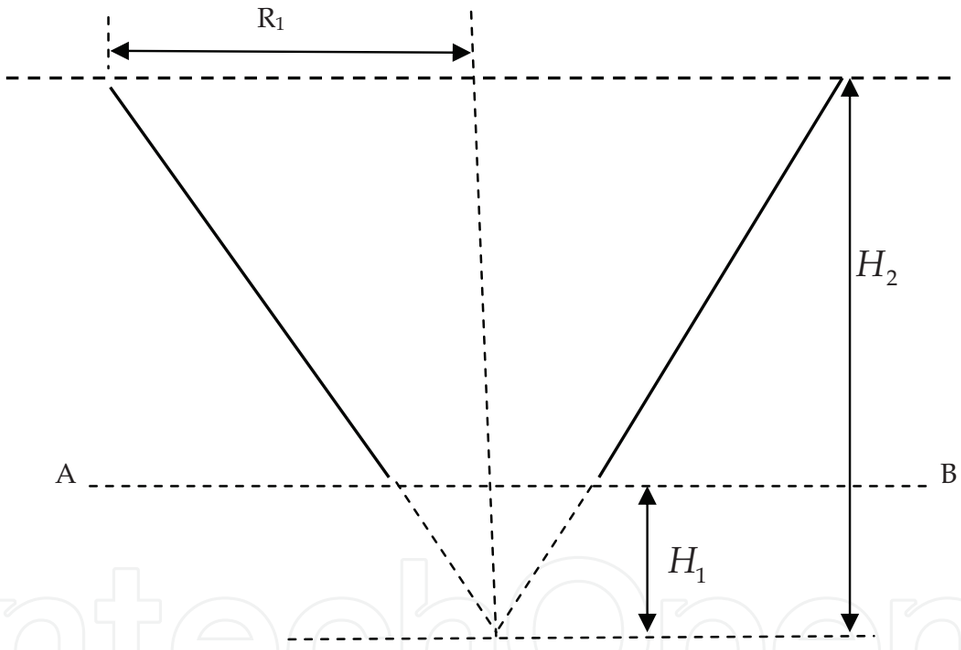

Fig. 3.1. *Schematic diagram of a cone showing the distance H_1 from the apex to the cross section AB (absorber area) and the distance H_2 from the apex to the collector area*

Suppose that a curve *AB* in the $xy-$plane like the one shown in Figure 3a is revolved about the $x-$axis to generate a surface. If *AB* is approximated by an inscribed polygon, then each segment *PQ* of the polygon will sweep out part of a cone whose axis lies along the $x-$axis (magnified view in Figure 3b). If the base radii of the *frustrum* of the cone are r_1 and r_2, as shown in Figure 3c, and its slant height is L, then its lateral surface area, A_r, is given as (Grant & Phillips, 1978)]
The total of the *frustrum* areas swept out by the segments of the inscribed polygon from *A* to *B* will give an approximate area *S* of the surface swept out by the curve *AB*. The approximation leads to an integral for *S* as follows.

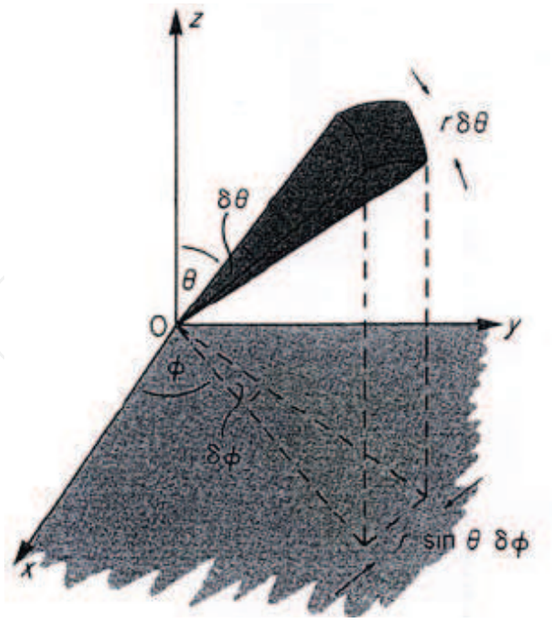

Fig. 3.2. *The cone subtends angles* $\delta\theta$ *and* $\delta\phi$ *at the origin, and its cross sectional area at a distance* r *from the apex is* $r^2 \sin\theta\delta\theta\delta\phi$ *.[1].*

If we let the coordinates P be (x, y) and Q be $(x+\Delta x, y+\Delta y)$, then the dimensions of the *frustrum* swept out by the line segment PQ are

$$r_1 = y\ ,\ r_2 = y + \Delta y \quad L = \sqrt{(\Delta x)^2 + (\Delta y)^2} \tag{3.5}$$

The lateral area of the *frustrum,* from Eq. (4), is

$$A = \pi(r_1 + r_2)L = \pi(2y + \Delta y)\sqrt{(\Delta x)^2 + (\Delta y)^2} \tag{3.6}$$

Adding the individual *frustrum* areas over the interval $[a.b]$ from left to right, we obtain

$$\text{Cone frustrum sum} = \sum_{x=a}^{b} \pi(2y + \Delta y)\sqrt{(\Delta x)^2 + (\Delta y)^2} \tag{3.7}$$

Eq. (3.7) can be rewritten as

$$\text{Cone frustrum sum} = \sum_{a}^{b} 2\pi\left(y + \frac{1}{2}\Delta y\right)\sqrt{1 + \left(\frac{\Delta y}{\Delta x}\right)^2} \tag{3.8}$$

Assuming y and dy/dx to be continuous functions of x, then the sum in Eq.(3.8) approaches a limit given as

$$S = \int_{a}^{b} 2\pi y\sqrt{1 + \left(\frac{dy}{dx}\right)^2}\, dx \tag{3.9}$$

We therefore define the area of the surface to be the value of this integral. Eq. (3.9) is easily remembered if we write

$$\sqrt{1+\left(\frac{dy}{dx}\right)^2}\,dx = ds \tag{3.10}$$

and take

$$S = \int 2\pi y ds \tag{3.11}$$

We interpret $2\pi y$ as the circumference and ds as the slant height. Thus $2\pi y ds$ gives the lateral area of a *frustrum* of cone of slant height ds if the point (x, y) is the midpoint of the element of arc length ds.

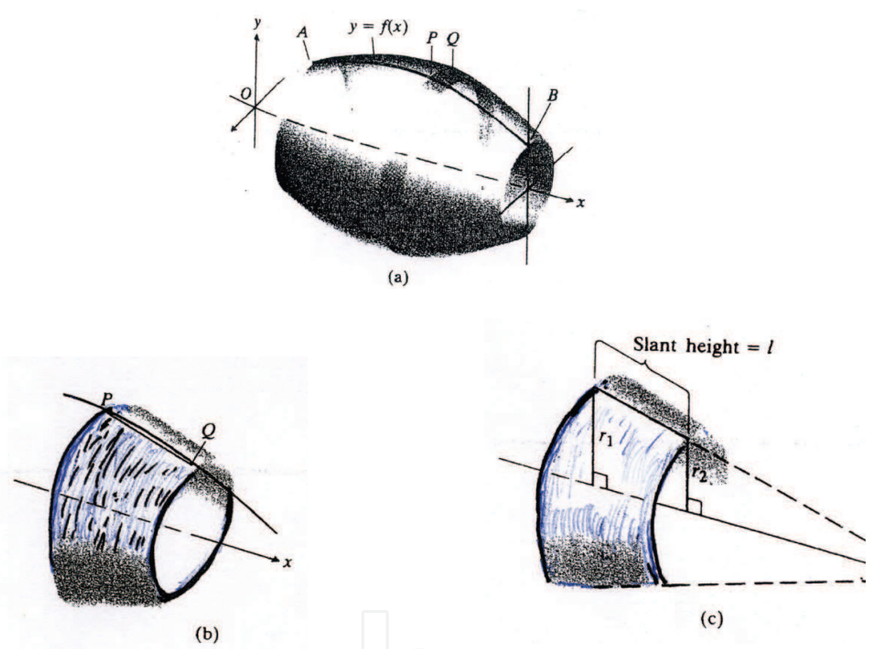

Fig. 3.3. *Generation of a cone from a curve AB by using frustrums as parts of the cone.*

4. Generating cone concentrators and collectors from hyperbloid configurations

The starting point of our analysis is based on the principles and operations of the cone concentrator. These principles are used to build on new systems when additional elements and components are added to modify the cone giving it two different configurations.

Figure 4.1 shows a parabolic compound concentrator (CPC) with axes of the two parabolas passing through the foci of the parabolas. We use these axes to generate a cone which embeds the parabola as shown in Figure 4.2. By drawing two lines parallel and passing through the foci of the first and second parabola, the lines meet at a point just below the foci. The two lines are then rotated along the axis of the compound parabola in order to form a

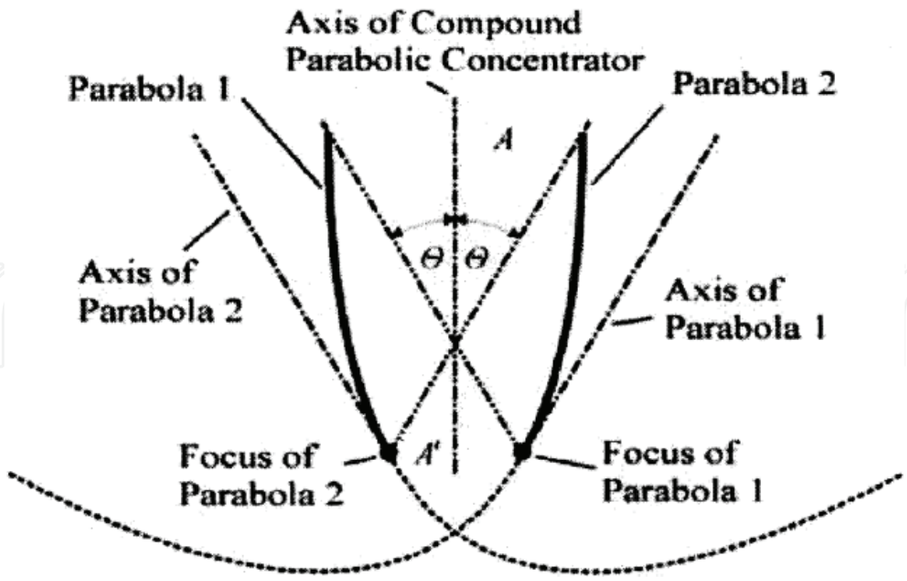

Fig. 4.1. *Compound parabolic concentrator (CPC).*

three dimensional straight cone. If the parabola embedded in Figure 2 is removed we remain with a cone having the same extreme angle as the original parabola provided the dimensions are not changed. A two dimensional schematic of such a cone generated in this manner is shown in Fig. 4.2.

If the cone as shown in Fig. 4.2 has a semi angle θ and θ_i is the extreme input angle, then the ray which enters at the extreme input angle will just pass through the aperture after one reflection if $2\theta = (\pi/2 - \theta_i)$. For a given entry diameter, an expression for the length of the cone can be obtained. It can be seen that some other rays such as the one indicated by the double arrow which enter at some angle less than the extreme input angle will be turned back by the cone. If a longer cone is used which has more reflections, some rays will still be turned back.

The cone is far from being an ideal concentrator. (Williamson, 1952) and (Witte, 1965) attempted some analysis of the cone concentrator by restricting their analysis to the meridian rays. The meridian ray analysis gives a very optimistic estimate of the concentrator; however, it does not address the problem of back reflections. Nevertheless, the cone is very simple compared to the image forming concentrators and its general form suggest a new direction in which to look for better concentrators. Modifications of the straight cone led to a Winston cone (http://scienceworld.wolfram.com/physics /WinstonCone.html), Hilderband and Winston, 1982), (Winston 1970), (Welford and Winston, 1989). A schematic of the Winston cone is shown in Fig. 4.3.

If an attempt is made to improve on the cone-concentrator by applying the edge-ray principle which stated loosely require that all extreme rays should form sharp image points and should emerge from the rim of the exit aperture, then one is led to the description of the Compound Parabolic Concentrator (CPC). These are prototypes of a series of nonimaging concentrators that approach very close to being ideal and having the maximum theoretical concentration ratio. Cones are much easier to manufacture than CPCs. Paraboloids of revolutions (which of course CPCs are not) seem a more natural choice to conventional physicists as concentrators.

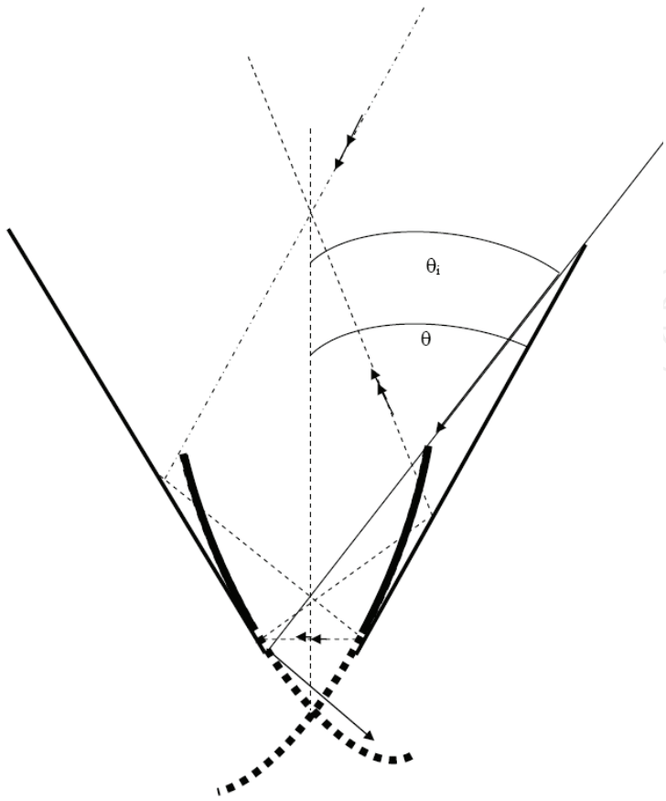

Fig. 4.2. *The cone concentrator with an "embedded" parabolic concentrator.*

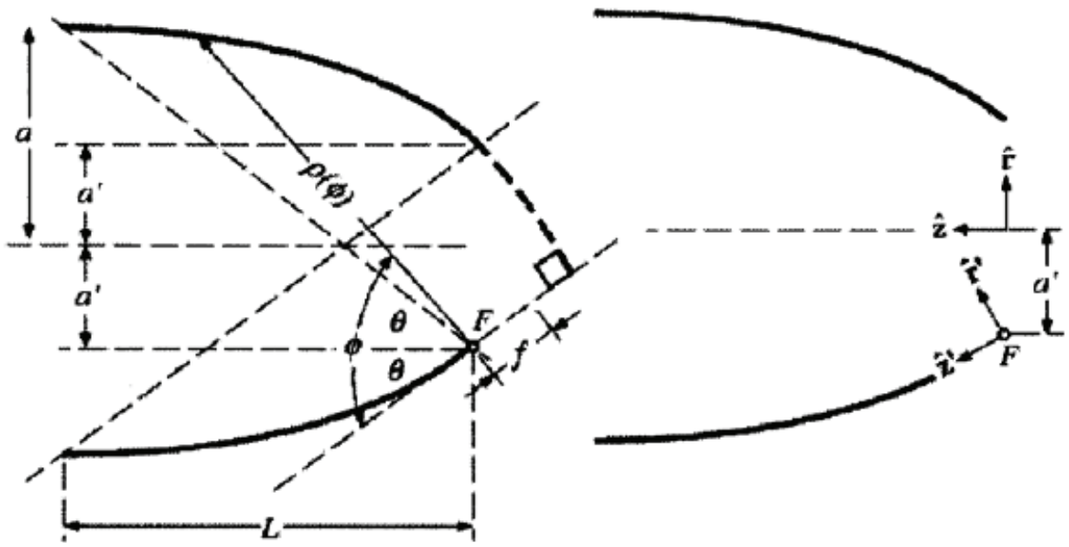

Fig. 4.3. *Winston cone concentrator.*

As a result of the foregoing, we consider two configuration models of modified cone concentrators as shown in Figure 5.1 and Figure 5.4 in which we analyze the systems by considering the heat exchange processes. We introduce a "reverse modelling technique" by creating certain components and elements in the design that will not only reduce the "back

reflections" but also increase the geometric concentration ratios of the systems. The introduction of an outer cylinder limits the extent of the entrance aperture to a certain value just like in the case of a fixed lens, which has a specific radius of curvature. The smaller cylinder and the bigger cylinder serve two other purposes. The first purpose is to guide the radiation on to the absorber and the second purpose is to reduce the size of the exit aperture, thus increasing the concentrations ratio.

In the first model of the concentrator shown in Figure 5.1, the system is made of polyvinyl (PVC) pipes of two different diameters that form the radiation guide to the copper ring which acts as an absorber. The collector is a cone also made of polyvinyl and has a base that fits exactly on top of the inner cylinder. The cone is glued on top of the smaller cylinder. The system of cone and two cylinders form the collector and concentrator. The system is placed on top of one of the copper rings depicted in Figure 5.2. The copper rings are made from a copper tube having very small thickness.

The copper rings are painted black to allow for maximum absorption of radiation from a halogen lamp for example, that is used to simulate solar radiation. The inside surface of the larger cylinder and the external surface of the smaller cylinder are painted with white barium sulphate paint to allow for maximum reflection of radiation.

Let I_D be the direct radiation from a halogen lamp for example, falling directly on one of the rings and let I_R be the radiation falling on the ring as a result of being collected on the surface of the cone and guided to the ring by the walls of the cylinder forming the guide. If I_T is the total radiation from the halogen lamp, then

$$I_T = I_D + I_R - L \tag{4.1}$$

where $L = l_c + l_r$. Here l_c represents the loss due reflections and radiation from the cone and the guide whereas l_r represents the loss of radiation from the ring.

Using Eq. (4.1), we can write the heat transfer / balance equations for the two systems (the open system and the concentrator) as:

$$I_D - l_r = m_w c_w \frac{dT_{open}}{dt} + m_c c_c \frac{dT_{open}}{dt} \tag{4.2}$$

where m_w is the mass of the water in the ring and c_w is the specific heat capacity of water while m_c is the mass of the copper ring and c_c is the specific heat capacity of copper. For the concentrator we can write the heat balance equation as

$$I_D + I_R - (l_c + l_r) = m_w c_w \frac{dT_{conc}}{dt} + m_c c_c \frac{dT_{conc}}{dt} \tag{4.3}$$

For the first configuration of the solar collector and concentrator (inverted cone) shown in Figure 5, one of the important relations is

$$S_1^2 = R_1^2 + H_1^2 , \tag{4.4}$$

The surface area of the cone according to Eq. (3.9) is therefore given by

$$A_s = \pi R_1 S_1 \tag{4.5}$$

where R_1 is the base radius, H_1 the vertical height and $\sqrt{R_1^2 + H_1^2} = S_1$ the slant height of the cone.

Equation (4.4) is true if we assume that the surface area of the cylinder enclosing the surface area of the cone does not participate in collecting the radiation, however, it does to some extent, therefore the total surface area of the cone and cylinder concerned with the collection of radiation may be written in the form

$$A_s = \pi R_1 S_1 + \pi \left(R_1 + d_1\right)^2 \mu H_1 \tag{4.6}$$

with the second term in Eq. (4.6) representing the surface area of the cylinder involved in collection of radiation. μ, whose value lies between 0 and 1, that is, $0 \le \mu \le 1$. $\mu = 0$ corresponds to the case in which the outer cylinder physically exists but only provides guiding of solar radiation down on to the absorber.

The surface area of the ring on which radiation falls is given as

$$A_{ring} = \pi \left(R_1 + d_1\right)^2 - \pi R_1^2, \tag{4.7}$$

and can be rewritten as

$$A_{ring} = \pi \left(d_1^2 + 2R_1 d_1\right). \tag{4.8}$$

The geometric concentration ratio in this configuration calculated by substituting Eq. (4.6) and Eq. (4.8) in to Eq. (2.1), results in

$$\left(CR_g\right)_1 = \frac{R_1 S_1 + (R_1 + d_1)^2 \mu H_1}{\left(d_1^2 + 2R_1 d_1\right)}. \tag{4.9}$$

which for $\mu = 0$ reduces to

$$\left(CR_g\right)_1 = \frac{R_1 S_1}{\left(d_1^2 + 2R_1 d_1\right)} \tag{4.10}$$

5. Experiment

Six (6) thermocouples T1, T2, T3, T4, T5, and T6 (Fig. 7) to measure temperatures of water in the rings with the concentrator and that without the concentrator are interfaced to a Fluke-2286/5 data logger through a temperature-measuring card attached to the data logger. Three of the thermocouples T1 T2 and T3 measure the temperature of the water in the ring with the concentrator while the other three thermocouples T4 T5 and T6 measure the temperature of the water in the ring without the concentrator.

In this work, both rings separated by a distance of 1.5 meters to avoid any effect of one ring on another are filled with water at the same temperature and the valves closed. The water remaining in the inlet is then drained and the two identical halogen lamps rated 90 watts powered by a 12 volt power source placed at the same height of 25cm from the rings are switched on simultaneously to heat the rings and thus, the water.

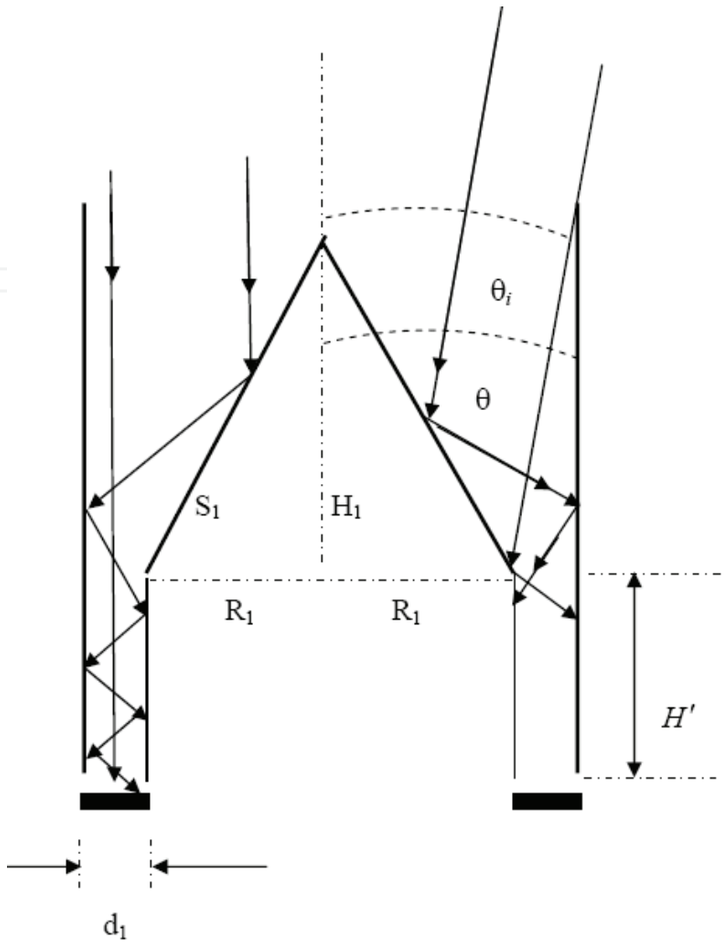

Fig. 5.1. *Vertical cross –section of the concentrator showing the path of both direct radiation collected by the cone absorber surface and guided to the ring by the radiation guide.*

The readings of the first three thermocouples are automatically averaged at pre-set time intervals and the resulting average value of the temperature stored in a specified register in the data logger. The other three thermocouples inserted into the ring not covered by the concentrator measure the temperature of water contained in the ring. The average temperature of the water is taken at the same pre-set time interval as that of the concentrator. The data logger (programmed using machine language) display on its output screen and print both the average temperature of the water in the ring with the concentrator and the average temperature of water in the ring without the concentrator.

Both copper tubes used to make the rings in the experiment had diameters of 0.01m. The height, H', of the radiation guide formed by the two cylinders was 10cm. The vertical height, H, of the cone used in this work was 0.2 cm.

Calculations done on the amount of heat reflected on the surface of the cone and inside the cylindrical guide show that if the initial radiation is reflected only once on the surface of the cone in to the radiation guide, then the guide will receive 98% of the original heat energy (http://www.oceanoptics.com/Products/ispref.asp, 2006)). Continuing the analysis on the 98% limit, a second reflected radiation inside the guide will posses 96.04% of the original radiation and a third beam reflected from the guide will have 94.12% of the original energy.

A fourth reflected beam possesses 92.24% of the initial radiation and a fifth reflected beam has 90.39% of the original radiation. Further analysis and simulation show that after several reflections from the surface of the cone through the radiation guide, the amount of radiation which will fall on the ring in this configuration is still more than 50% of the original radiation. Figure 5.5 shows the curve obtained from simulation of the remaining energy versus the number of reflections (Ochieng *et. al.* 2007). It is thus reasonable to assume that

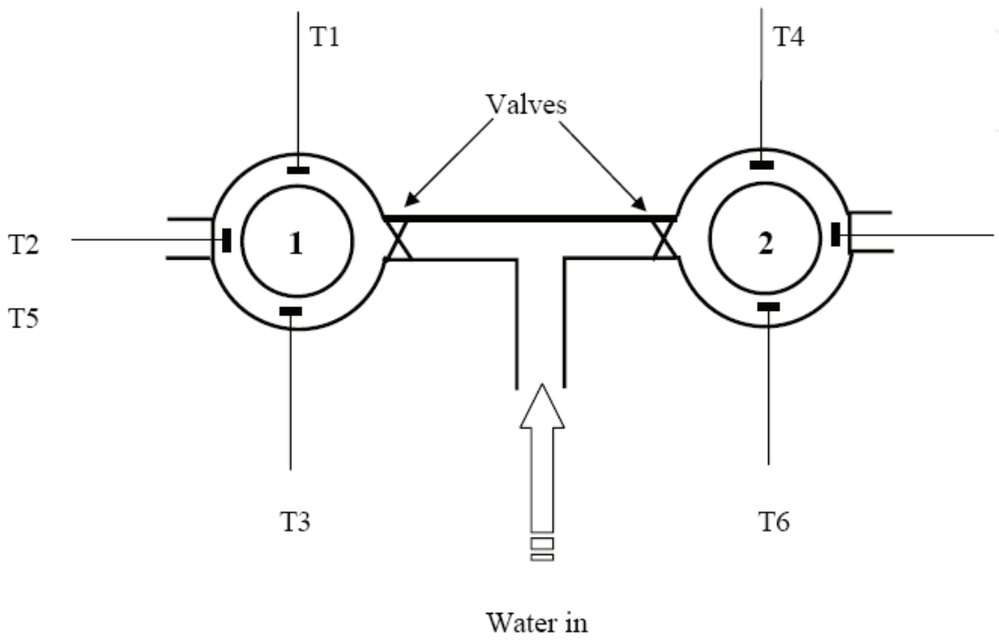

Fig. 5.2. *Arrangement of the rings and thermocouples for solar water heater experiment.*

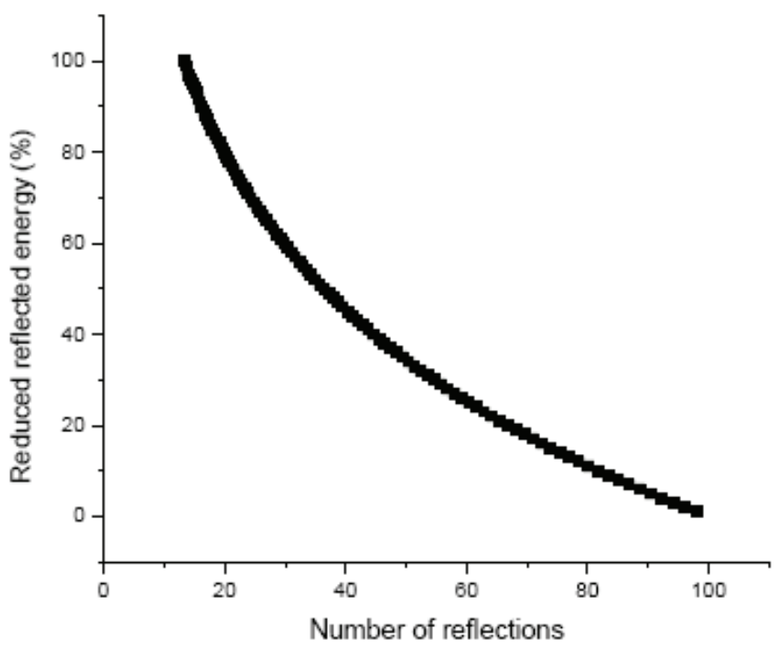

Fig. 5.3. *Reflected energy versus the number of reflections.*

the ring in the concentrator is heated by the radiation coming directly from the halogen lamp as well as by some radiation collected on the surface of the cone and guided to the ring by the walls of the cylinders forming the guide.

In this section we analyze and calculate the concentration ratio of a modified cone shown in Figure 8. This cone has an axial cylinder whose exterior surface area is considered to be involved in solar radiation collection.

If the modified cone concentrator has an axial cylinder as shown in Fig. 5.4, then the axial cylinder can also be taken to aid in radiation collection. Hence, the total area of solar collector in a modified cone concentrator can be written as

$$A_{coll} = \pi R_x \sqrt{\left[R_2 - \left(l_2 + d_2\right)\right] + H_2^2} + 2\pi l_2 H_2 \beta \tag{5.1}$$

where $R_x = R_2 - (l_2 + d_2)$ and $\sqrt{\left[\left(R_2 - (l_2 + d_2)\right)\right]^2 + H_2^2}$ is the slant height, S_2, of the modified cone concentrator

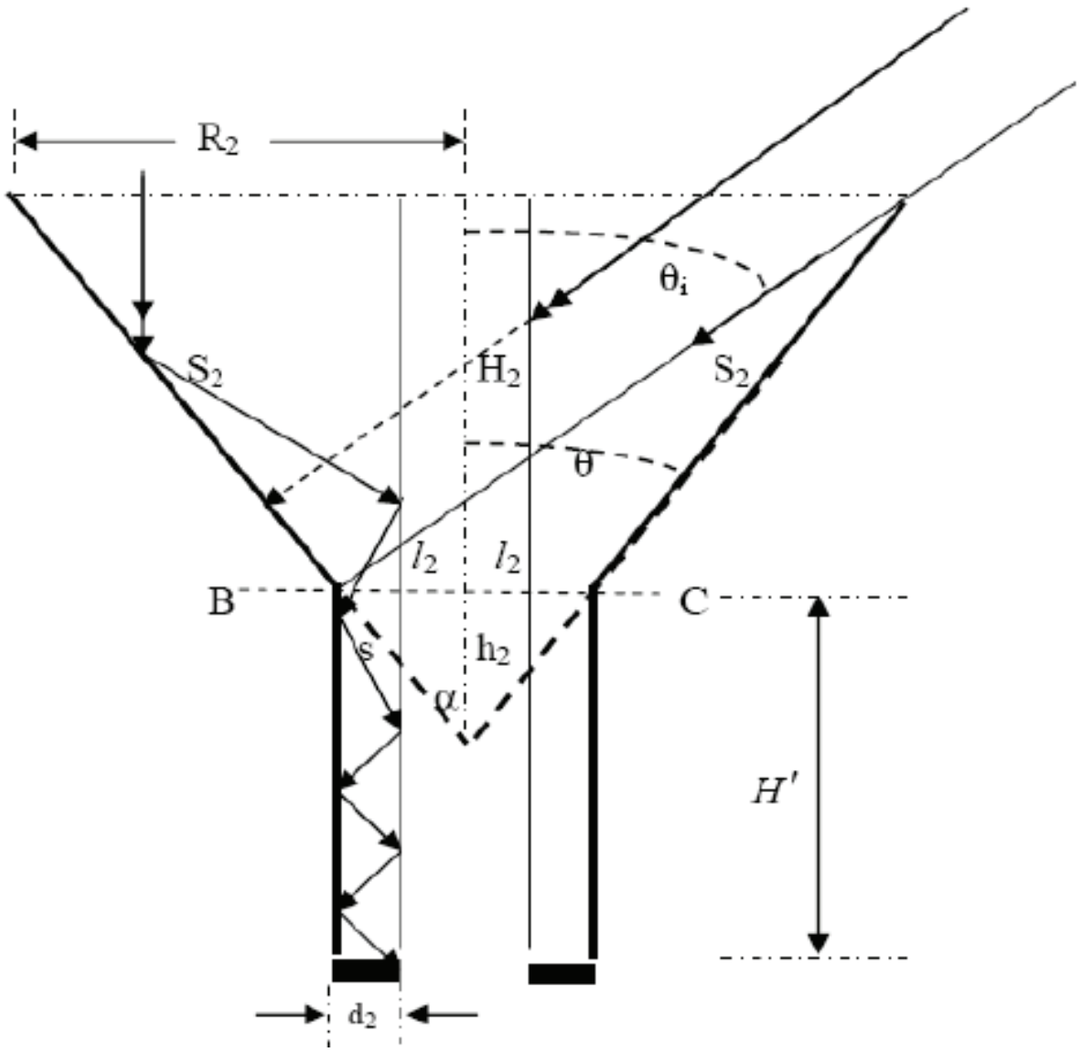

Fig. 5.4. *A modified cone concentrator with an axial cylinder, which also aids in radiation collection.*

The absorber surface area of the modified cone concentrator is then given by

$$A_{abs} = \pi\left(2l_2 d_2 - 2d_2^2\right) \tag{5.2}$$

Thus, the expression for the geometric concentration ratio of the modified cone concentrator according to the configuration of Fig. 8 is given by

$$\frac{A_{coll}}{A_{abs}} = \frac{R_x\left(\sqrt{\left(R_2 - \left(l_2 + d_2\right)\right)^2 + H_2^2}\right) - l_2\sqrt{l_2^2 + h_2^2} + 2\left(l_2 - d_2\right)^2 H_2\beta}{\left(\frac{d_2}{2}\right)^2} \tag{5.3}$$

It has also been assumed in this configuration that the axial cylinder is involved in the collection of radiation, hence the factor β indicate the percentage of its surface area involved in the collection of solar radiation. $0 \le \beta \le 1$, where $\beta = 0$ has the physical meaning that the external surface area of the axial cylinder is not part of the collection area of solar radiation.

6. Results

Fig.6.1 show results obtained for the experimental set up shown in Fig. 5.2 in which the concetrator configuration of Fig. 5.4 was used.

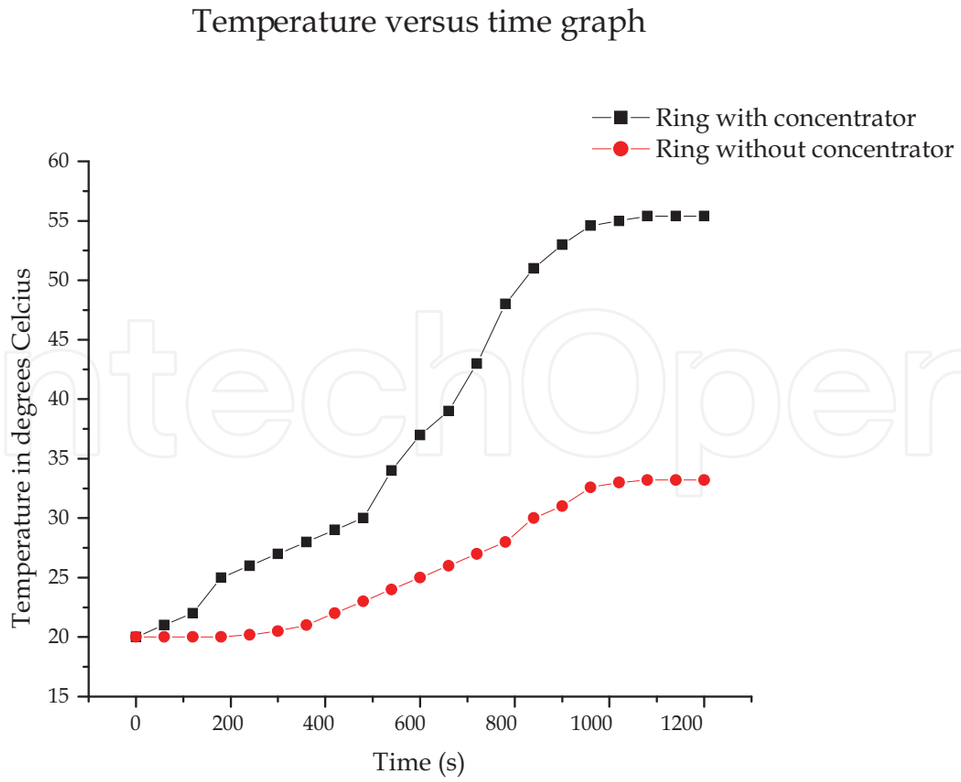

Fig. 6.1. *Curves for heating water in an open ring and in a cone-cylinder concentrator.*

The figure show curves obtained for the temperature of water in the ring with the concentrator and the ring without the concentrator as functions of time using the model of Fig.8. It was also found that the water in the ring with the concentrator rose to more than 55.4^{o}C after being exposed to the radiation for a period of 1,200 seconds while water in the ring without the concentrator reached a temperature of 33.2^{o}C for the same exposure time of 1,200 seconds to radiation. The water in the ring with the concentrator thus attained a higher temperature than the water in the ring without the concentrator (open ring).

Using models in which the dimensions given hold, theoretical geometric concentration ratios of different configurations of cones and cone-cylinder combinations concentrators with modifications were calculated: $H_2 = 2$ m, $H_1 = h_2 = 0.5$ m, $d_2 = 0.01$ m $R_1 = R_2 = 1$ m, $d_1 = 0.04$ m, $S_1 = S_2 = 2.69$ m, $l_2 = 0.228$ m . For the given dimensions, our results show that for a straight cone as shown in Fig. 3.1, the geometric concentration ratio is found to be 16 by employing Eq. (3.3). The value for $S_1 = S_2 = 2.69$ m is calculated from the values of $H_1, H_2\ R_1$ and R_2 . The geometric concentration ration of the concentrator shown in Fig. 5 calculated using Eq. (4.10) is found to be 33.33. With $\beta = 1$ in Eq. 5.1, the theoretical concentration ratio of the configuration works out to be 90,400.

Concentrator	Description of concentrator	Theoretical value of geometric concentration ratio
Figure 3.1	Cone concentrator (Using Eq. 3.3)	16.00
	(Using Eq. 2.1)	19.10
Figure 5.1	Inverted cone-cylinder concentrator with a radiation guide and outer cylinder	33.33
Figure 5.4	Straight cone concentrator with radiation guide and axial cylinder	90,400
Figure 5.4	Straight cone concentrator with radiation guide but no axial cylinder $(\beta = 0)$	90,000

Table 1. Summary of results of theoretical geometric concentration ratios for different configurational geometries of cone, cone-cylinder concentrators.

7. Discussion

The results obtained in this work show that a mathematical procedure can be used to calculate the effective collector and absorber surface areas of cone concentrators. The technique can be extended to a modified cone concentrator and the values obtained for the ratio of the collector to the absorber area of the concentrator give the geometric concentration ratio. Though this method gives the correct values of concentration ratios, just as the inverse sine of the acceptance angle method, both do not present any idea on the size or configurational geometry of the system.

It can be seen from this work that configurational geometry of cone and cone cylinder-combinations of concentrators give different theoretical geometric concentration ratios for the same dimensions. Additional components are seen to improve the geometric concentration ratio.

8. Conclusion

The work shows that for a straight cone with a collector area A_{coll} ,situated a distance H_2 from the apex and an absorber area, A_{abs} , at a distance H_1 from the apex, the ratio of the squares of H_2 to H_1 give the geometric concentration ratio of the cone concentrator. The geometric concentration ratio has been calculated using configurational geometry giving the same value when the dimensions of the cone are used. The method of using the ratio of the squares of the heights can therefore be used as a quick way of approximation of the concentration ratio of a straight cone without taking many measurements.

No literature exist for the solar concentrator shown in Fig. 5.1 that have been reported in this work except for the work by (Ochieng and Onyango, 2009). However, variants of this concentrator such as the straight cone type in which some literature can be found, (Williamson, 1952), (Witte, 1965), (Smith, 1966), (Welford and Wilson, 1978). The inclusion of cylindrical component is a completely a new addition. There is therefore need to build prototypes and test them with actual solar radiation. The values of the theoretical geometric concentrations can be raised by making the denominator in Eq. (4.10), and Eq. (5.1) smaller. Two possible ways of doing this are: (1) to reduce the diameter of the copper ring but keep the other dimensions of the concentrator constant and (2) to increase the surface area of the cone but keep the other parameters of the concentrator constant.

As can be seen from Figure 6.1, the rise in temperature of water in the open ring seems to be gradual while that of the ring with the concentrator is steeper. A possible explanation of this effect is that the water in the ring with the concentrator is heated by direct radiation from the halogen lamp as well as by the radiation collected on the surface of the cone which is guided on to the ring by the cylinder walls whereas in the open ring, the heating only takes place by the direct radiation from the lamp. It can also be noted that in the open ring, energy loss is due to two processes, namely radiation and convection while the ring in the concentrator may loose little energy by convection because it is almost a closed system.

As in the straight cone, both configurations discussed in this work have semi angles denoted by θ . The extreme angle is denoted by θ_i . It can be seen from Figure 5.4 that some of the radiation enter through the angle less than θ_i that would have been "back-reflected" are multiply reflected from the surface of the axial cylinder and the surface of the cone in to the radiation guide and end on the absorber. The amount of radiation that will not be "back-reflected" can be calculated by determining the shading by the axial cylinder on to the surface of the cone.

All the radiation, axial and off axis in the inverted cone concentrator of Figure 5.1 end up on the absorber. However, it is easy to see that by making the cone angle bigger; the cone becomes flatter and tends to a flat plate collector in which case not all the radiation falling on its surface will be channeled in to the guide.

One of the advantages of using the configuration of Figure 5.4 rather than that of Figure 5.1 for a solar collector concentrator is that the surface area of the cone can be increased easily without affecting the other dimensions of the system just by increasing the slant height S_2. If an attempt is made to do the same thing with the other configuration (Figure 5.1) by keeping the cone angle constant, bigger cylinders forming the radiation guide must be used. This, however, has a counterproductive effect of increasing the surface area of the absorber and thus reducing the geometric concentration ratio.

Since actual systems have not been constructed and tested, there are many parameters that can be varied in order to find out appropriate dimensions for such systems which maximize

the geometric concentration ratio. These parameters include the height H' of the radiation guide, the base radius R, the slant height S, and the vertical height H of the cone.
The reason for suggesting changing H' to a smaller value say by an amount δ, is that the area on which radiation will be lost through the guide will change from $\pi H\left(d^2+2Rd\right)$ to $\pi\left[H-\delta\right]\left(d^2+2Rd\right)$. Since $H-\delta < H$, a smaller area will be available for radiation loss inside the guide. PVCs were preferred in this work because they are poor conductors of heat.

9. References

Basset, I.M., and Derrick, G.H. (1978). The collection of diffuse light into an extended absorber. *Optical and Quantum Electronics* 10, 61-82.

Burkhard, D.G., and Shealy, D.L. (1975). Design of reflectors which distribute sunlight in a specific manner. *Sol. Energy* 17, 221-227.

Cornbleet, S. (1976). *Microwave Optics*. Academic Press, New York.

Garg, H.P., and Kandpal, T.C. (1999), *Laboratory Manual on Solar Thermal Experiments.*, Narosa, New Delhi, ISBN 81-7319-340-1

Grant, I.S., and Phillips, W.R., (1978*). Electromagnetism*, John Wiley and Sons, ISBN 0 471 99707 2, Great Britain.

Hildebrand, R.H., and Winston, R. (1982), Throughput of Diffraction-Limited Field Optics System for Infrared and Millimetric Telescope. *Appl. Opt*. 21, 1844-1846.

Hinterberger, H., and Wilson, R. (1968a). Use of a solid light funnel to increase phototube aperture without restricting angular acceptance. *Rev. Sci. Instr*. 39, 1217-1218.

Hotler, M.L., Nudelman, S., Suits, G.H., Wolf, W.L., and Zissis, G.J. (1962*), Fundamentals of Infrared Technology*, Macmillan, New York.

Maatouk, K., and Shigenao, M. (2005). Theoretical approach of a flat plate solar collector with clear and low-iron glass covers taking into account the spectral absorption and emission within glass cover layers. *Renewable Energy.* 30, 1177-1194. http://www.oceanoptics.com/Products/ispref.asp (2006)).

Morgan, S.P. (1958). General solutions of the Luneburg lens problem. *J. Appl. Phys*. 29, 1358-1368.

Ochieng R M and Onyango F N. A new type of solar concentrator employing a cone-cylinder combination, International Journal of Global Energy Issues, Vol. 31, No. 2, 169-182. 2009, ISSN (Print) 0954-7118, (Online) 1741-5128.

Ochieng, R.M., Onyango, F.N., and Owino, A.J. (2007), Determination of global absorptivity and emissivity of some opaque bulk materials using an integrating sphere calorimeter without ports. *Meas. Sci. Technol*. 18, 2667-2672, ISSN 0975-0233. dio:10.1088/0957-0233/18/8/043

Rabl, A., and Winston,R., (1976), Ideal concentrators for finite sources and restricted exit angles, *Appl. Opt.* 15, 2880-2883.

Rabl, A., (1976a), Solar concentrators with maximal concentration for cylinder absorbers, *Appl. Opt.* 15, 1871-1873.

Rabl, A., (1976b), Comparison of solar thermal concentrators, *Sol. Energy* 18, *93-111.*

Rabl, A., (1976c), Optical and thermal properties of compound parabolic concentrators, *Sol. Energy* 18, 497-511.

Welford, W.T., and Winston, R (1978), *The Optics of Nonimaging Concentrators-Light and Solar Energy*, Academic Press, New York.

Williamson, D. E., (1952), Cone channel condensed optics, *J. Opt. Soc. Amer*. 42, 712-715.

Witte, W., (1965), Cone channels optics, *Infrared Phys*. 5, 197-185.

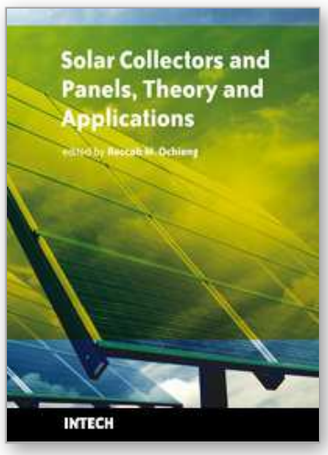

Solar Collectors and Panels, Theory and Applications

Edited by Dr. Reccab Manyala

ISBN 978-953-307-142-8
Hard cover, 444 pages
Publisher Sciyo
Published online 05, October, 2010
Published in print edition October, 2010

This book provides a quick read for experts, researchers as well as novices in the field of solar collectors and panels research, technology, applications, theory and trends in research. It covers the use of solar panels applications in detail, ranging from lighting to use in solar vehicles.

How to reference

In order to correctly reference this scholarly work, feel free to copy and paste the following:

Reccab Manyala and Frederick Onyango (2010). Some Techniques in Configurational Geometry as Applied to Solar Collectors and Concentrators, Solar Collectors and Panels, Theory and Applications, Dr. Reccab Manyala (Ed.), ISBN: 978-953-307-142-8, InTech, Available from: http://www.intechopen.com/books/solar-collectors-and-panels--theory-and-applications/some-techniques-in-configurational-geometry-as-applied-to-solar-collectors-and-concentrators

INTECH
open science | open minds

InTech Europe
University Campus STeP Ri
Slavka Krautzeka 83/A
51000 Rijeka, Croatia
Phone: +385 (51) 770 447
Fax: +385 (51) 686 166
www.intechopen.com

InTech China
Unit 405, Office Block, Hotel Equatorial Shanghai
No.65, Yan An Road (West), Shanghai, 200040, China
中国上海市延安西路65号上海国际贵都大饭店办公楼405单元
Phone: +86-21-62489820
Fax: +86-21-62489821

© 2010 The Author(s). Licensee IntechOpen. This chapter is distributed under the terms of the Creative Commons Attribution-NonCommercial-ShareAlike-3.0 License, which permits use, distribution and reproduction for non-commercial purposes, provided the original is properly cited and derivative works building on this content are distributed under the same license.

IntechOpen

IntechOpen